

## An in situ neutron diffraction study of cation disordering in synthetic qandilite $\text{Mg}_2\text{TiO}_4$ at high temperatures

HUGH ST. C. O'NEILL,<sup>1</sup> SIMON A. T. REDFERN,<sup>1,2,\*</sup> SUE KESSON,<sup>1</sup> AND SIMINE SHORT<sup>3</sup>

<sup>1</sup>Research School of Earth Sciences, Australian National University, Canberra, ACT 0200, Australia

<sup>2</sup>Department of Earth Sciences, University of Cambridge, Downing Street, Cambridge CB2 3EQ, U.K.

<sup>3</sup>Intense Pulsed Neutron Source, Argonne National Laboratory, 9700 South Cass Avenue, Argonne, Illinois 60439-4814, U.S.A.

### ABSTRACT

Temperature-dependent cation order-disorder has been studied in many 2+ – 3+ oxide spinels but 4+ – 2+ spinels have been found to be either completely normal or completely inverse when examined at room temperature. Here we report the temperature dependence of the cation distribution in the 4–2 spinel synthetic qandilite ( $\text{Mg}_2\text{TiO}_4$ ) from in situ time-of-flight neutron powder diffraction experiments to 1416 °C. At room temperature,  $\text{Mg}_2\text{TiO}_4$  is confirmed to have completely inverse cation distribution, with Ti atoms occupying half the octahedrally coordinated cation sites. Cation disordering becomes observable above about 900 °C, with 4% of the Ti occupying the tetrahedral site by 1416 °C. The rate of reordering on cooling is fast, such that high-temperature disorder is not preserved on cooling to room temperature. The thermodynamics of the change in cation distribution with temperature can be described by an enthalpy of Mg–Ti disorder of  $-46.1 \pm 0.4$  kJ/mol.

### INTRODUCTION

The oxide spinels comprise a structural class that includes several rock-forming minerals. End-member spinels have the formula  $\text{AB}_2\text{O}_4$ , where, usually, either A is a divalent and B a trivalent cation, or A is a quadravalent and B is a divalent cation. These types are known as 2–3 and 4–2 spinels respectively (other types, such as the spinel form of  $\text{Na}_2\text{WO}_4$  with a 1–6 cation content, are also known). Examples of 2–3 spinels are the minerals spinel sensu stricto ( $\text{MgAl}_2\text{O}_4$ ), chromite ( $\text{FeCr}_2\text{O}_4$ ), and magnetite ( $\text{Fe}_3\text{O}_4$ , i.e.,  $\text{Fe}^{2+}\text{Fe}_2^{3+}\text{O}_4$ ). Examples of 4–2 spinels are found in nature somewhat less commonly, but include the important minerals ringwoodite ( $\gamma\text{-Mg}_2\text{SiO}_4$ , the most abundant phase in the lower part of the transition zone of the Earth's mantle) and ulvospinel,  $\text{Fe}_2\text{TiO}_4$ . Another mineral with the 4–2 spinel-structure is the magnesium equivalent of ulvospinel, the rare mineral  $\text{Mg}_2\text{TiO}_4$ , which has been given the name qandilite (Al-Hermezi 1985; Oktyabrsky et al. 1992).

One well-known feature of spinel crystal chemistry is the temperature-dependent disordering of the A and B cations between the octahedrally and tetrahedrally coordinated sites. This cation order-disorder may influence many of the physical properties of a spinel crystal; for example, the magnetic properties of the ferrite spinels (2–3 spinels with  $\text{B} = \text{Fe}^{3+}$ ) are particularly sensitive to their cation distribution. Cation order/disorder also contributes to the free energy of a spinel, hence its stability. To describe this cation order-disorder, the formula of a spinel may be written  $(\text{A}_{1-x}\text{B}_x)^{\text{tet}}[\text{A}_x\text{B}_{2-x}]^{\text{oct}}\text{O}_4$ , where  $x$  is called the inversion parameter. If  $x$  is 0, the cations are completely ordered onto the two cation sites; the structural formula is  $(\text{A})^{\text{tet}}[\text{B}_2]^{\text{oct}}\text{O}_4$ , and the spinel is said to have the “normal” cation distribution. The opposite extreme occurs if  $x$  is 1, cor-

responding to  $(\text{B})^{\text{tet}}[\text{AB}]^{\text{oct}}\text{O}_4$ , in which case the spinel is said to have the “inverse” cation arrangement. With increasing temperature there will be a tendency for both normal and inverse spinels to disorder toward the random, maximum entropy, cation arrangement, at  $x = 2/3$ . The relationship between order-disorder and temperature has been studied experimentally in many 2–3 spinels, both on samples quenched from high temperature, and, more recently, directly at temperature, using powder neutron diffraction (e.g., Peterson et al. 1991; Redfern et al. 1999; Harrison et al. 1998).

However, no study on the temperature dependence of the cation distribution in a 4–2 spinels has hitherto been attempted, probably because quenched samples of 4–2 spinels are either completely normal (i.e.,  $x = 0$  within experimental error), or completely inverse ( $x = 1$ ). The completely normal 4–2 species include the silicate and germanate spinels ( $\text{M}_2\text{SiO}_4$  and  $\text{M}_2\text{GeO}_4$ , where  $\text{M} = \text{Mg} \pm \text{Fe}^{2+}$ ), whereas the titanates, stannates, and all other 4–2 spinels have the inverse arrangement.

There are two possible reasons for the apparent lack of cation disorder in quenched 4–2 spinels: either these spinels simply do not show measurable disorder up to their melting temperatures (e.g.,  $\text{MgCr}_2\text{O}_4$  among the 2–3 spinels, see O'Neill and Dollase 1994), or some disordering does occur, but the kinetics of reordering are so fast that the disorder cannot be preserved on quenching. With the prospect of performing measurements directly at temperature by powder neutron diffraction, it should now be possible to distinguish between these two alternatives. The importance of even a small amount of order-disorder in ringwoodite ( $\gamma\text{-Mg}_2\text{SiO}_4$ ) to its stability relations was pointed out by Navrotsky (1977), and has more recently been discussed by Hazen et al. (1993).

$\text{Mg}_2\text{TiO}_4$  (synthetic qandilite) is a good choice for a first test of whether 4–2 spinels might show high-temperature cation order-disorder, as there is a large difference in the neutron

\* E-mail: satr@esc.cam.ac.uk

scattering lengths of Mg ( $b = 5.375$  fm) and Ti ( $b = -3.438$  fm), such that neutron diffraction methods can pick up small changes in  $x$ , on the order of 0.003 (see below). The pure stoichiometric phase is readily synthesized in sufficient quantities for powder neutron diffraction work. Mg<sub>2</sub>TiO<sub>4</sub> remains stable to high temperatures (it melts incongruently to MgO plus liquid at 1756 °C, according to Woermann et al. 1969), and should show minimal changes in stoichiometry due to either volatilization of its constituent oxides, or oxidation state, over a wide range of O atom fugacities. This is important experimentally, as reliable results can be anticipated without precise control of O atom fugacity (in contrast to Fe<sub>2</sub>TiO<sub>4</sub>, for example). Although there are two putative complications, that Mg<sub>2</sub>TiO<sub>4</sub> breaks down to MgO + MgTiO<sub>3</sub> at or slightly below 1000 °C (Akimoto and Syono 1967; Millard et al. 1995), and also transforms (presumably metastably, in light of the above observation) to a tetragonal modification of the spinel structure at temperatures below about 933 ± 20 K (Wechsler and Navrotsky 1984), these do not cause practical problems, as the rates of transformation are too sluggish to occur during a typical diffraction experiment. The structure of Mg<sub>2</sub>TiO<sub>4</sub> at room temperature has been determined previously by Wechsler and von Dreele (1989) by powder neutron diffraction; by Millard et al. (1995) by powder X-ray diffraction; and by Sawada (1996) by single-crystal X-ray diffraction using a flux-grown sample.

### EXPERIMENTAL METHODS

A ceramic sample of Mg<sub>2</sub>TiO<sub>4</sub> weighing 15 g was synthesized from MgO (99.999%) and TiO<sub>2</sub> (99.8%). The oxides were dried at 1100 °C, weighed, and thoroughly mixed by grinding under acetone in an agate mortar. The mixture was pelletized using a 0.5 inch tungsten carbide dye. Pellets were placed on a sheet of platinum, and sintered in a box furnace at 1400 °C in air for 52 hours. The pellets were cooled to room temperature by removing them from the furnace (i.e., the quench was not particularly fast).

A small chip of one of the pellets was lightly ground for examination by powder XRD, using a Siemens D-5005, CoK $\alpha$  radiation, with the addition of an internal standard of NIST Si ( $a_0 = 5.431195$  Å). Data were collected from 15 to 135° 2 $\theta$ . The sample was found to be single-phase spinel, with a lattice parameter of 8.4419(2) Å, in excellent agreement with Millard et al. (1995), who obtained 8.4418 Å. The sample was further characterized by Rietveld refinement of powder XRD data collected both with and without the Si internal standard (Table 1), using the DBWS program (Young et al. 1995).

High-temperature neutron powder diffraction data were collected using the special environment powder diffractometer (SEPD) time-of-flight instrument at the Intense Pulsed Neutron Source (IPNS), Argonne National Laboratory, U.S.A. (Jorgensen et al. 1989). The sintered pellets of Mg<sub>2</sub>TiO<sub>4</sub> were loaded into the furnace as a self-supporting stack and held in place by a weighted plunger. The furnace was evacuated to prevent oxidation of the furnace elements.

Diffraction patterns were collected over flight times corresponding to  $d$ -spacings between 0.4 and 3.2 Å, with total counting times of about 40 minutes per pattern. Data were collected at intervals after both heating and cooling. In the first cycle,

**TABLE 1.** Rietveld refinement of powder XRD data from Mg<sub>2</sub>TiO<sub>4</sub>

NIST Si std (111) excluded	present no	present yes	absent no	absent yes
Profile function	pseudo Voigt	pseudo Voigt	pseudo Voigt	pseudo Voigt
Displacement	0.013(1)	0.014(1)	0.043(1)	0.047(2)
Transparency	0.053(1)	0.052(1)	0.049(2)	0.044(2)
% Mg <sub>2</sub> TiO <sub>4</sub>	73	73	100	100
$a_0$ (Å)	8.44192(5)	8.44189(5)	8.44105(7)	8.44094(4)
$U$ O atom	0.2594(1)	0.2597(2)	0.2590(1)	0.2608(2)
$U$	0.0051(10)	0.0032(12)	0.0096(8)	0.0061(9)
$V$	0.0144(16)	0.0177(22)	-0.0008(15)	0.0063(18)
$W$	0.0073(5)	0.0056(8)	0.01522(6)	0.0117(8)
% Lorentzian	88(1)	91(1)	75(1)	79(1)
$B_{so}$ tetrahedral	0.67(5)	0.68(5)	0.25(4)	0.34(4)
$B_{so}$ octahedral	0.58(3)	0.59(3)	0.17(3)	0.24(3)
$B_{so}$ O atom	0.81(3)	0.79(6)	0.72(5)	0.67(5)
$\chi^2$	1.49	1.47	1.50	1.41
$R_{Bragg}$ spinel (%)	3.8	4.1	4.2	3.7
$R_{Bragg}$ Si (%)	1.7	1.6		

Note: CoK $\alpha$  radiation,  $\alpha_2:\alpha_1 = 0.5$ ,  $\lambda_{\alpha_1} = 1.78890$  Å,  $\lambda_{\alpha_2} = 1.79280$  Å, 18.5–130° 2 $\theta$ , stepsize 0.02, 9 s/step, zero-background quartz plate, with 2 rad/s rotation.

the sample was heated in steps to 1054 °C, at which temperature the sample fell over, necessitating that the furnace be returned to room temperature, the sample replaced, and the experiment started again. In the second cycle, data were collected in steps on heating to 1416 °C (approximately the high-temperature limit of the furnace) and then on cooling back to near room temperature, without mishap. An important observation is that the sample pellets were recovered at the end of this experiment with the same white color as they started out with, indicating negligible reduction in the inert atmosphere of the furnace (Mg<sub>2</sub>TiO<sub>4</sub> readily turns black on slight reduction of Ti<sup>4+</sup> to Ti<sup>3+</sup>).

Refinements of the neutron diffraction data were carried out using the GSAS Rietveld package, adopting chemical constraints on the total Mg and Ti contents over the A and B sites. The results are given in Table 2. Isotropic temperature factors were used for all atoms. Initially attempts were made to refine these independently, but since scattering at the B site is very low, with positive scattering from Mg being compensated by negative scattering from Ti, we adopted a further constraint. The ratio of  $U_{iso}$  for the A and B sites was, therefore, held constant. The background was modeled by a shifted Chebyshev six-term function. Data were refined until convergence. Further details of the refinement procedure are given in Table 3, and a typical fitted pattern is shown in Figure 1.

### RESULTS

The results from the refinements of the high-temperature neutron diffraction experiments are given in Table 2, in the order in which the measurements were made. In agreement with the previous neutron diffraction study (Wechsler and Von Dreele 1989), we find that Mg<sub>2</sub>TiO<sub>4</sub> is completely inverse at room temperature [ $x = 1.000(3)$ ], but begins to show a small amount of disorder at ~900 °C, rising to nearly 4% [ $x = 0.960(4)$ ] at the highest temperature attempted in the experiment, 1416 °C (Fig. 2). The change in  $x$  is completely reversed on cooling.

**TABLE 2.** Refined structural parameters for Mg<sub>2</sub>TiO<sub>4</sub> from neutron diffraction experiments

<i>T</i> (°C)	<i>a</i> (Å)*	<i>x</i>	<i>ut</i>	<i>U</i> <sub>60tet</sub> (nm <sup>2</sup> )	<i>U</i> <sub>60oct</sub> (nm <sup>2</sup> )	<i>U</i> <sub>60ox</sub> (nm <sup>2</sup> )	<i>R</i> <sub>wp</sub>
<b>First series</b>							
90	8.4469	0.995(3)	0.2610	0.26(4)	0.27(4)	0.49(2)	0.093
70	8.4456	0.993(3)	0.2610	0.19(4)	0.20(4)	0.47(2)	0.105
97	8.4474	0.994(3)	0.2610	0.21(4)	0.22(4)	0.48(2)	0.106
152	8.4520	0.996(3)	0.2609	0.36(4)	0.37(5)	0.56(2)	0.102
220	8.4578	0.997(3)	0.2610	0.37(4)	0.39(5)	0.63(2)	0.101
289	8.4638	0.999(3)	0.2610	0.48(5)	0.50(5)	0.68(2)	0.097
360	8.4698	0.997(3)	0.2611	0.62(5)	0.66(5)	0.75(3)	0.098
425	8.4757	0.998(3)	0.2611	0.66(5)	0.69(5)	0.83(3)	0.095
483	8.4816	0.993(3)	0.2611	0.71(5)	0.75(5)	0.91(3)	0.093
559	8.4877	0.995(3)	0.2611	0.82(6)	0.86(6)	0.98(3)	0.092
625	8.4941	0.994(3)	0.2610	0.90(6)	0.95(6)	1.06(3)	0.090
690	8.5008	0.995(3)	0.2611	1.02(6)	1.07(6)	1.14(3)	0.089
756	8.5073	0.994(3)	0.2611	1.10(6)	1.15(6)	1.17(3)	0.087
820	8.5140	0.992(3)	0.2611	1.17(6)	1.23(7)	1.27(3)	0.086
885	8.5208	0.985(3)	0.2611	1.29(7)	1.35(7)	1.39(3)	0.084
949	8.5277	0.989(3)	0.2611	1.47(7)	1.54(7)	1.46(3)	0.083
1020	8.5353	0.986(3)	0.2610	1.42(7)	1.49(8)	1.55(4)	0.088
1054	8.5389	0.988(7)	0.2612	1.83(17)	1.92(18)	1.61(8)	0.163
<b>Second series</b>							
100	8.4510	1.004(4)	0.2609	0.60(6)	0.63(6)	0.55(3)	0.087
240	8.4561	1.002(4)	0.2609	0.71(6)	0.75(7)	0.64(3)	0.089
559	8.4872	0.998(4)	0.2610	1.14(8)	1.19(8)	1.02(3)	0.085
850	8.5154	0.998(4)	0.2610	1.47(8)	1.54(9)	1.31(4)	0.082
912	8.5224	0.993(4)	0.2611	1.63(10)	1.71(9)	1.42(4)	0.081
975	8.5287	0.991(4)	0.2611	1.64(10)	1.72(10)	1.48(4)	0.096
1039	8.5367	0.989(4)	0.2610	1.73(9)	1.82(9)	1.56(4)	0.082
1103	8.5442	0.985(4)	0.2611	1.81(9)	1.90(10)	1.66(4)	0.079
1167	8.5519	0.986(4)	0.2611	1.94(10)	2.04(10)	1.70(4)	0.080
1232	8.5597	0.978(4)	0.2611	1.90(9)	1.99(10)	1.78(4)	0.078
1297	8.5674	0.980(4)	0.2612	2.08(10)	2.19(10)	1.87(4)	0.078
1359	8.5754	0.967(4)	0.2610	2.18(10)	2.29(11)	2.00(5)	0.079
1403	8.5814	0.968(4)	0.2611	2.48(11)	2.60(11)	2.06(5)	0.075
1416	8.5820	0.960(4)	0.2612	2.46(11)	2.58(11)	2.08(5)	0.075
1397	8.5807	0.964(4)	0.2611	2.43(11)	2.55(11)	2.03(5)	0.076
1346	8.5735	0.972(4)	0.2610	2.20(10)	2.30(11)	1.91(5)	0.076
1283	8.5661	0.975(4)	0.2612	2.13(10)	2.24(11)	1.85(4)	0.077
1219	8.5586	0.980(4)	0.2611	2.04(10)	2.14(11)	1.78(4)	0.079
1081	8.5413	0.979(4)	0.2611	1.90(10)	1.99(10)	1.66(4)	0.079
944	8.5275	0.989(4)	0.2610	1.66(9)	1.74(9)	1.46(4)	0.083
882	8.5199	0.993(4)	0.2610	1.57(9)	1.65(9)	1.35(4)	0.081
797	8.5110	0.995(4)	0.2610	1.43(8)	1.50(9)	1.27(4)	0.082
756	8.5075	1.000(4)	0.2610	1.46(8)	1.53(9)	1.21(4)	0.083
693	8.5011	1.000(4)	0.2610	1.25(8)	1.31(8)	1.11(4)	0.086
630	8.4947	0.999(4)	0.2610	1.23(8)	1.30(8)	1.06(4)	0.090
567	8.4886	0.997(4)	0.2610	1.16(8)	1.22(8)	1.00(3)	0.089
503	8.4828	1.003(4)	0.2609	1.05(7)	1.10(8)	0.91(3)	0.090
439	8.4769	1.002(4)	0.2609	0.99(7)	1.03(8)	0.85(3)	0.092
375	8.4716	0.997(4)	0.2610	0.88(7)	0.93(7)	0.78(3)	0.094
312	8.4661	1.003(4)	0.2609	0.82(7)	0.86(7)	0.72(3)	0.097
250	8.4612	1.002(4)	0.2608	0.71(7)	0.75(7)	0.65(3)	0.099
198	8.4569	1.002(4)	0.2608	0.64(6)	0.67(7)	0.61(3)	0.099
168	8.4545	1.007(4)	0.2608	0.59(8)	0.62(8)	0.56(4)	0.138

Note: *R*<sub>wp</sub> is defined as  $\sqrt{\frac{\sum w(I_o - I_c)^2}{\sum wI_o^2}}$ .

The room-temperature cell parameters have been calibrated against a second measurement employing an internal Si standard.

\* ± 0.0001 Å.

† ± 0.0001.

The observation that the sample has a completely inverse distribution initially despite its preparation at 1400 °C suggests that the rate of cation reordering in Mg<sub>2</sub>TiO<sub>4</sub> is too rapid to be quenched in. Rapid kinetics would explain why previous investigations of Mg<sub>2</sub>TiO<sub>4</sub> at room temperature (and also other 4–2 spinels) have always found negligible disorder.

The temperature evolution of the lattice parameter is shown in Figure 3. The volume thermal expansivity of Mg<sub>2</sub>TiO<sub>4</sub> was obtained by fitting all the lattice parameter data simultaneously. Because small changes in sample position between the first and second series of measurements resulted in a small offset in the measured cell parameter we assumed different values of

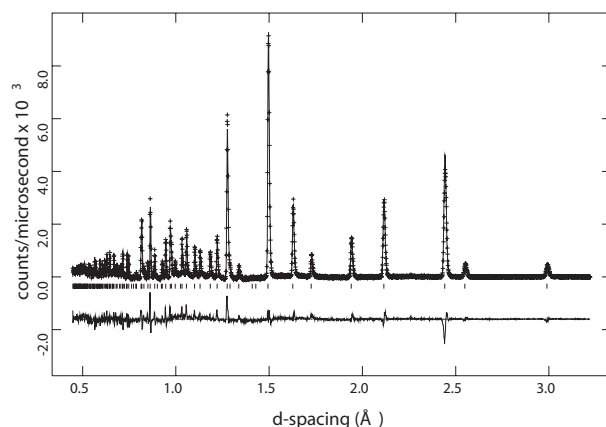
$V_{(298.15\text{ K})}^0$ , the molar volume at standard temperature and pressure, for the first and second series of measurements, and fitted all data by least squares regression to the expression:

$$V_{(T)}^0 = V_{(298.15\text{ K})}^0 [1 + \sum_{n \geq 1} \alpha_n (T - 298.15)^n] \quad (1)$$

with  $\alpha_1 = 2.89 \times 10^{-5}$ ,  $\alpha_2 = 2.58 \times 10^{-9}$ , and  $\alpha_3 = 2.18 \times 10^{-12}$ . The quality of the fit is very sensitive to the value assumed for the uncertainty in temperature, which is not really well known, a priori. Assuming an uncertainty in *T* of 4 K returns a reduced chi-squared ( $\chi^2_\nu$ ) of 1.4 for the regression, implying that this value is appropriate. The first two data from the second series

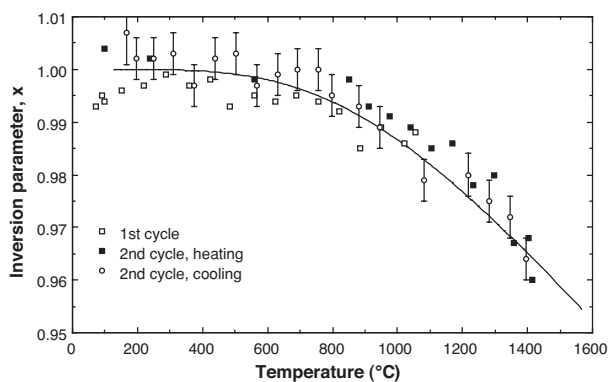
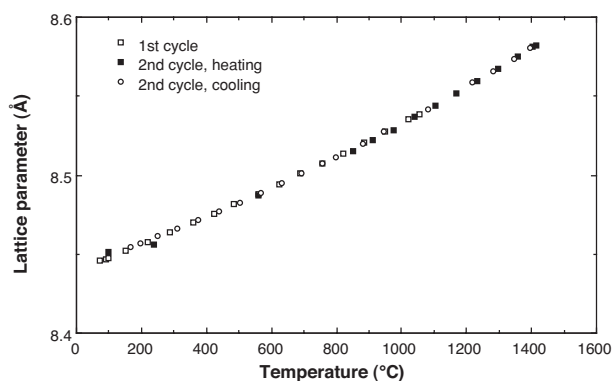
**TABLE 3.** Experimental and instrumental parameters pertaining to the Rietveld refinements of data collected at the Intense Pulsed Neutron Source (IPNS), Argonne National Laboratory

Instrumental	
Diffractometer	SEPD (neutron time-of-flight powder diffractometer)
Moderator	100 K liquid methane
Flight path	Moderator-sample = 14 m, Sample-detector = 1.5 m
Detector	40 × 10 atm <sup>3</sup> He proportional counters at ± 90°
Data range	2507.5 to 17998.5 μs
Time channel binning	Δd/d = 0.0054
Temperature	See Table 2
Refinement	
Space group	<i>Fd3m</i>
Unit cell refinement	Whole pattern
Observations	2214
Number of observed reflections	199
Refined parameters	
Structural	5
Profile	3
Background	6-term Chebyshev polynomial of the first kind
Cell	
Constraints	1
Strict ( <i>U</i> <sub>iso</sub> )	Mg1 = Ti1 = 1.05(Mg2 = Ti2)
Strict (Ssite = 1)	Mg1 + Ti1, Mg2 + Ti2, Mg1 + Mg2, Ti1 + Ti2
Thermal parameters	
Agreement factors	All atoms isotropic
	See Table 2

**FIGURE 1.** Refined neutron diffraction pattern for synthetic qandilite at 289 °C. Crosses indicate data points (background subtracted), solid line indicates fit.

(i.e., those at 100 and 240 °C) are obviously anomalous (most likely due to a difference between the thermocouple and sample temperature) and were excluded from the regression, leaving 49 data for the fit. The value of  $V_{(298.15\text{ K})}^0$  from the powder XRD measurement is 45.288 cm<sup>3</sup>.

The cubic term (in  $\alpha_3$ ) is statistically significant only if the data above 1000 °C are included; thus it may reflect the onset of cation disordering, implying that molar volume increases with decreasing  $x$ . This means that pressure would tend to suppress the disordering in this sample. But the data are not sufficient for this to be a firm conclusion. Determining the volume

**FIGURE 2.** Temperature dependence of the inversion parameter for synthetic qandilite, from neutron diffraction refinements. The solid line shows the fit to the data using our thermodynamic model for ordering. The uncertainties in the data are of the same order of magnitude for all three data sets. For clarity error bars are only shown for the cooling cycle.**FIGURE 3.** Temperature dependence of the lattice parameter of synthetic qandilite. The uncertainties in the data are of the same order of magnitude for all three data sets and are smaller than the symbols.

change with cation distribution is one area in which measurements from quenched samples can have an advantage over in situ measurements, since, with measurements from quenched samples, any change of volume with cation distribution is not obscured by the concurrent thermal expansivity. From inspection of the experimental data, at  $T > 900$  °C it appears that cation inversion,  $x$ , shows an inverse relation with cell parameter  $a$ . This is exactly the same behavior as one would expect at room temperature: due to the different cation radii assumed by Mg and Ti<sup>4+</sup> at the T and M sites of the spinel structure, a decrease of inversion in Mg<sub>2</sub>TiO<sub>4</sub> is expected to cause a decrease of the T-O distance and an increase of the M-O distances. As a consequence of the geometrical relations between polyhedral site sizes and the cell parameter of the spinel structure, M sites are much more influential on the cell parameter than T sites. Increments in the M-O bond length lead to cell enlargements. This effect, due to disorder, is an important contribution to the increase of the  $a$  parameter and may thus explain the slight change of slope observed at  $T > 900$  °C (Fig. 3).

The O atom positional parameter ( $u$ ) shows a very slight increase with temperature (Fig. 4). This is only observable be-

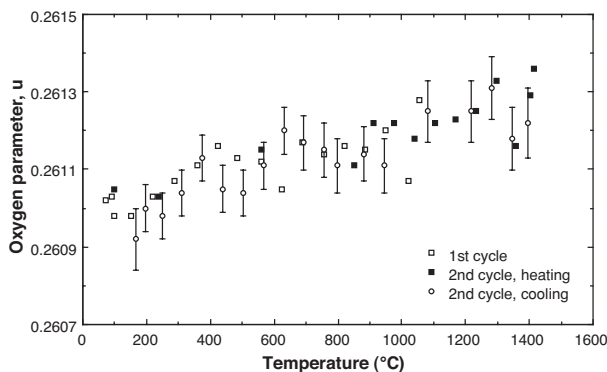


**FIGURE 4.** Temperature dependence of the O atom positional parameter,  $u$ , for synthetic qandilite. The weak monotonic increase with temperature demonstrates the weak coupling to disordering. The uncertainties in the data are of the same order of magnitude for all three data sets. For the sake of clarity error bars are only shown for the cooling cycle.

cause  $u$  is determined very precisely in neutron diffraction experiments. Regression of all data gives

$$u = 0.26094 + 1.99 \times 10^{-7} T \text{ (K)} \quad (2)$$

The increase in  $u$  is monotonic over the temperature range of the measurements, in contrast to the change in  $x$ , which only decreases from unity above  $\sim 900$  °C. The lack of correspondence in the changes of  $u$  and  $x$  with temperature implies that the change in  $u$  is due only to the different thermal expansivities of the tetrahedral and octahedral coordination polyhedra (Fig. 5). One must also bear in mind that the variation in  $x$ , while measurable, is none the less only very small, and can only be expected to have a small effect on  $u$ . Our observed value of  $u$  at room temperature (25 °C) is 0.2610(2). Given the apparent precision, this is in only fair agreement with the previous neutron diffraction measurement of Wechsler and von Dreele (1989) of 0.26049(3), or with the single-crystal XRD value of 0.26072(5) of Sawada (1996). The powder XRD refinement of Millard et al. (1995) gave 0.2616(1), and our own XRD powder refinement of the data collected without added Si (Table 1) gave 0.2590(1). The reason for the anomalously low value from our powder refinement is probably associated with surface roughness of the sample, which can act to decrease the relative intensity of low angle reflections by absorption. The intensity of the strong low angle reflection (111) in  $\text{Mg}_2\text{TiO}_4$  is very sensitive to the  $u$  parameter. For example, we find that by simply omitting the 111 reflection from refinement of the X-ray data increases  $u$  to 0.2608(2), a value in good agreement with our neutron data.

#### THERMODYNAMIC MODELING

O'Neill and Navrotsky (1983) showed from lattice energy arguments that the change in enthalpy of a spinel as a function of the cation distribution parameter,  $x$ , was expected to have a quadratic form, i.e.,  $\Delta H(x) = \alpha x + \beta x^2$ . Combining this with the configurational entropy of the spinel as a function of  $x$ , gives the expression for the free energy of the spinel relative to a

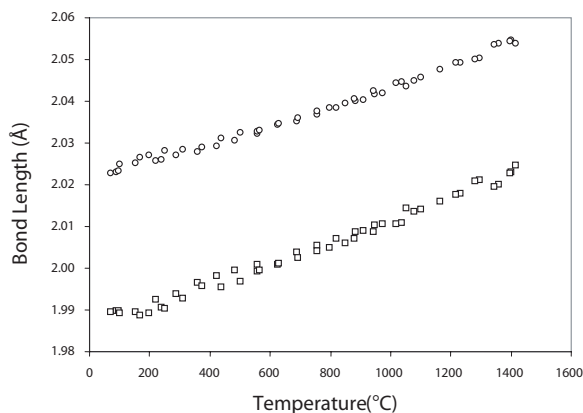


**FIGURE 5.** Temperature dependence of the T-O (tetrahedral, shown as squares) and M-O (octahedral, shown as circles) bond lengths in qandilite.

standard state of the perfectly normal spinel ( $x = 0$ ):

$$\Delta G(x) = \alpha x + 2\beta x^2 + RT \left( \sum_{M,b} n_b X_M^b \ln X_M^b \right) \quad (3)$$

where  $X_M^b$  is the fraction of cations of type M in site b. For an end-member spinel, the values of  $X_M^b$  are simple functions of  $x$ . At equilibrium, the free energy is at a minimum [ $\partial \Delta G(x) / \partial x = 0$ ], hence:

$$RT \ln \left( \frac{x^2}{(1-x)(2-x)} \right) = \alpha + 2\beta x \quad (4)$$

The amount of disorder shown by  $\text{Mg}_2\text{TiO}_4$  in the present work is too small to constrain accurately both the  $\alpha$  and the  $\beta$  parameters in equation 4. Putting  $\beta = 0$ , we obtain  $\alpha = -46.1 \pm 0.4$  kJ/mol, with  $\chi^2 = 1.06$ , indicating an excellent fit, as illustrated in Figure 2.

#### DISCUSSION

O'Neill and Navrotsky (1983) showed empirically that the magnitude of the  $\beta$  term in 2–3 spinels was about  $-20$  kJ/mol, from the published data available at that time on cation disorder as a function of temperature. Subsequent experimental work has shown that the  $\beta$  term cannot be treated as a constant common to all 2–3 spinels, as assumed (for convenience) by O'Neill and Navrotsky (1983). In particular, neutron diffraction work has shown that  $\beta$  is positive in  $\text{MgAl}_2\text{O}_4$  and  $\text{FeAl}_2\text{O}_4$  (Redfern et al. 1999; Harrison et al. 1998). Nevertheless, values near  $-20$  kJ/mol have been found for many 2–3 spinels.

O'Neill and Navrotsky (1983) then used lattice energy arguments to postulate that the  $\beta$  term should be about three to five times larger for 4–2 spinels. Taking into account that the lattice energy model overestimates energy effects, they suggested that the  $\beta$  term for 4–2 spinels should be about  $-60$  kJ/mol. A  $\beta$  term of this magnitude was found to model the solvus between the normal 4–2 spinel  $\text{Co}_2\text{GeO}_4$  and the inverse 4–2 spinel  $\text{Co}_2\text{TiO}_4$  quite satisfactorily (O'Neill and Navrotsky 1984). We emphasize that the present results do not exclude non-zero values of the  $\beta$  parameter; this remains unresolved.

The amount of disorder in  $\text{Mg}_2\text{TiO}_4$  at  $\sim 1400$  °C is 4%,

which is the same as that inferred by Hazen et al. (1993) from the Si-O bond distance for a sample of  $\gamma$ -Mg<sub>2</sub>SiO<sub>4</sub> synthesized at 1400 °C and 20 GPa. In Mg<sub>2</sub>TiO<sub>4</sub>, this amount of disorder corresponds to an entropy increase of 1.4 kJ/mol compared to the perfectly inverse cation distribution ( $x = 1$ ). Given the small changes in entropy generally associated with solid-solid phase transitions in the mantle, even entropy increments of this magnitude may have significant effects on the  $P$ - $T$  slopes of phase transitions, as pointed out by Navrotsky (1977).

### ACKNOWLEDGMENTS

The authors are grateful for the comments of two anonymous referees. This work benefited from the use of the Intense Pulsed Neutron Source at Argonne National Laboratory, which is funded by the U.S. Department of Energy, BES-Materials Science, under Contract W-31-109-ENG-38

### REFERENCES CITED

- Akimoto, S. and Syono, Y. (1967) High-pressure decomposition of some titanate spinels. *The Journal of Chemical Physics*, 47, 1813–1817.
- Al-Hermezi, H.M. (1985) Qandilite, a new spinel end-member, Mg<sub>2</sub>TiO<sub>4</sub>, from the Qala-Dizeh region, NE Iraq. *Mineralogical Magazine*, 49, 739–744.
- Harrison, R.J., Redfern, S.A.T., and O'Neill, H.S.C. (1998) The temperature dependence of the cation distribution in synthetic hercynite (FeAl<sub>2</sub>O<sub>4</sub>) from in-situ neutron structure refinements. *American Mineralogist*, 83, 1092–1099.
- Hazen, R.M., Downs, R.T., Finger, L.W., and Ko, J. (1993) Crystal chemistry of ferromagnesian silicate spinels: evidence for Mg-Si disorder. *American Mineralogist*, 78, 1320–1323.
- Jorgensen, J.D., Faber, J., Carpenter, J.M., Crawford, R.K., Haumann, J.R., Hitterman, R.L., Kleb, R., Ostrowski, G.E., Rotella, F.J., and Worlton, T.G. (1989) Electronically focussed time-of-flight powder diffractometers at the intense pulsed neutron source. *Journal of Applied Crystallography*, 22, 321–333.
- Millard, R.L., Peterson, R.C., and Hunter, B.K. (1995) Study of the cubic to tetragonal transition in Mg<sub>2</sub>TiO<sub>4</sub> and Zn<sub>2</sub>TiO<sub>4</sub> spinels by <sup>17</sup>O MAS NMR and Rietveld refinement of X-ray diffraction data. *American Mineralogist*, 80, 885–896.
- Navrotsky, A. (1977) Calculation of effect of cation disorder on silicate spinel phase boundaries. *Earth and Planetary Science Letters*, 33, 437–442.
- O'Neill, H.S.C. and Dollase, W.A. (1994) Crystal structures and cation distributions in simple spinels from powder XRD structural refinements: MgCr<sub>2</sub>O<sub>4</sub>, ZnCr<sub>2</sub>O<sub>4</sub>, Fe<sub>3</sub>O<sub>4</sub> and the temperature dependence of the cation distribution in ZnAl<sub>2</sub>O<sub>4</sub>. *Physics and Chemistry of Minerals*, 20, 541–555.
- O'Neill, H.S.C. and Navrotsky, A. (1983) Simple spinels: crystallographic parameters, cation radii, lattice energies and cation distribution. *American Mineralogist*, 68, 181–194.
- (1984) Cation distributions and thermodynamic properties of binary spinel solid solutions. *American Mineralogist*, 69, 733–753.
- Oktyabrsky, R.A., Shcheka, S.A., Lennikov, A.M., and Afanasyeva, T.B. (1992) The 1st occurrence of qandilite in Russia. *Mineralogical Magazine*, 56, 385–389.
- Peterson, R.C., Lager, G.A., and Hitterman, R.L. (1991) A time-of-flight neutron powder diffraction study of MgAl<sub>2</sub>O<sub>4</sub> at temperatures up to 1273 K. *American Mineralogist*, 76, 1455–1458.
- Redfern, S.A.T., Harrison, R.J., O'Neill, H.S.C., and Wood, D.R.R. (1999) Thermodynamics and kinetics of cation ordering in MgAl<sub>2</sub>O<sub>4</sub> spinel up to 1600 °C from in situ neutron diffraction. *American Mineralogist*, 84, 299–310.
- Sawada, H. (1996) Electron density study of spinels: magnesium titanium oxide (Mg<sub>2</sub>TiO<sub>4</sub>). *Materials Research Bulletin*, 31, 355–360.
- Wechsler, B.A. and Navrotsky, A. (1984) Thermodynamics and structural chemistry of compounds in the system MgO-TiO<sub>2</sub>. *Journal of Solid State Chemistry*, 55, 165–180.
- Wechsler, B.A. and Von Dreele, R.B. (1989) Structure refinement of Mg<sub>2</sub>TiO<sub>4</sub>, MgTiO<sub>3</sub> and MgTi<sub>2</sub>O<sub>5</sub> by time-of-flight neutron powder diffraction. *Acta Crystallographica*, B45, 542–549.
- Woermann, E., Brezney, B., and Muan, A. (1969) Phase equilibria in the system MgO-iron oxide-TiO<sub>2</sub> in air. *American Journal of Science*, 267, 463–479.
- Young, R.A., Sakthivel, A., Moss, T.S., and Paiva-Santos, C.O. (1995) DBWS-9411, an upgrade of the DBWS\* programs for Rietveld refinement with PC and mainframe computers. *Journal of Applied Crystallography*, 28, 366–367.

MANUSCRIPT RECEIVED JUNE 7, 2002

MANUSCRIPT ACCEPTED DECEMBER 2, 2002

MANUSCRIPT HANDLED BY BRYAN CHAKOUMAKOS